B meson decays to charmless meson pairs containing η or η' mesons

B. Aubert,[1] Y. Karyotakis,[1] J. P. Lees,[1] V. Poireau,[1] E. Prencipe,[1] X. Prudent,[1] V. Tisserand,[1] J. Garra Tico,[2] E. Grauges,[2] M. Martinelli,[3a,3b] A. Palano,[3a,3b] M. Pappagallo,[3a,3b] G. Eigen,[4] B. Stugu,[4] L. Sun,[4] M. Battaglia,[5] D. N. Brown,[5] L. T. Kerth,[5] Yu. G. Kolomensky,[5] G. Lynch,[5] I. L. Osipenkov,[5] K. Tackmann,[5] T. Tanabe,[5] C. M. Hawkes,[6] N. Soni,[6] A. T. Watson,[6] H. Koch,[7] T. Schroeder,[7] D. J. Asgeirsson,[8] B. G. Fulsom,[8] C. Hearty,[8] T. S. Mattison,[8] J. A. McKenna,[8] M. Barrett,[9] A. Khan,[9] A. Randle-Conde,[9] V. E. Blinov,[10] A. D. Bukin,[10,*] A. R. Buzykaev,[10] V. P. Druzhinin,[10] V. B. Golubev,[10] A. P. Onuchin,[10] S. I. Serednyakov,[10] Yu. I. Skovpen,[10] E. P. Solodov,[10] K. Yu. Todyshev,[10] M. Bondioli,[11] S. Curry,[11] I. Eschrich,[11] D. Kirkby,[11] A. J. Lankford,[11] P. Lund,[11] M. Mandelkern,[11] E. C. Martin,[11] D. P. Stoker,[11] H. Atmacan,[12] J. W. Gary,[12] F. Liu,[12] O. Long,[12] G. M. Vitug,[12] Z. Yasin,[12] V. Sharma,[13] C. Campagnari,[14] T. M. Hong,[14] D. Kovalskyi,[14] M. A. Mazur,[14] J. D. Richman,[14] T. W. Beck,[15] A. M. Eisner,[15] C. A. Heusch,[15] J. Kroseberg,[15] W. S. Lockman,[15] A. J. Martinez,[15] T. Schalk,[15] B. A. Schumm,[15] A. Seiden,[15] L. Wang,[15] L. O. Winstrom,[15] C. H. Cheng,[16] D. A. Doll,[16] B. Echenard,[16] F. Fang,[16] D. G. Hitlin,[16] I. Narsky,[16] P. Ongmongkolkul,[16] T. Piatenko,[16] F. C. Porter,[16] R. Andreassen,[17] G. Mancinelli,[17] B. T. Meadows,[17] K. Mishra,[17] M. D. Sokoloff,[17] P. C. Bloom,[18] W. T. Ford,[18] A. Gaz,[18] J. F. Hirschauer,[18] M. Nagel,[18] U. Nauenberg,[18] J. G. Smith,[18] S. R. Wagner,[18] R. Ayad,[19,†] W. H. Toki,[19] R. J. Wilson,[19] E. Feltresi,[20] A. Hauke,[20] H. Jasper,[20] T. M. Karbach,[20] J. Merkel,[20] A. Petzold,[20] B. Spaan,[20] K. Wacker,[20] M. J. Kobel,[21] R. Nogowski,[21] K. R. Schubert,[21] R. Schwierz,[21] D. Bernard,[22] E. Latour,[22] M. Verderi,[22] P. J. Clark,[23] S. Playfer,[23] J. E. Watson,[23] M. Andreotti,[24a,24b] D. Bettoni,[24a] C. Bozzi,[24a] R. Calabrese,[24a,24b] A. Cecchi,[24a,24b] G. Cibinetto,[24a,24b] E. Fioravanti,[24a,24b] P. Franchini,[24a,24b] E. Luppi,[24a,24b] M. Munerato,[24a,24b] M. Negrini,[24a,24b] A. Petrella,[24a,24b] L. Piemontese,[24a] V. Santoro,[24a,24b] R. Baldini-Ferroli,[25] A. Calcaterra,[25] R. de Sangro,[25] G. Finocchiaro,[25] S. Pacetti,[25] P. Patteri,[25] I. M. Peruzzi,[25,‡] M. Piccolo,[25] M. Rama,[25] A. Zallo,[25] R. Contri,[26a,26b] E. Guido,[26a,26b] M. Lo Vetere,[26a,26b] M. R. Monge,[26a,26b] S. Passaggio,[26a] C. Patrignani,[26a,26b] E. Robutti,[26a] S. Tosi,[26a,26b] K. S. Chaisanguanthum,[27] M. Morii,[27] A. Adametz,[28] J. Marks,[28] S. Schenk,[28] U. Uwer,[28] F. U. Bernlochner,[29] V. Klose,[29] H. M. Lacker,[29] T. Lueck,[29] A. Volk,[29] D. J. Bard,[30] P. D. Dauncey,[30] M. Tibbetts,[30] P. K. Behera,[31] M. J. Charles,[31] U. Mallik,[31] J. Cochran,[32] H. B. Crawley,[32] L. Dong,[32] V. Eyges,[32] W. T. Meyer,[32] S. Prell,[32] E. I. Rosenberg,[32] A. E. Rubin,[32] Y. Y. Gao,[33] A. V. Gritsan,[33] Z. J. Guo,[33] N. Arnaud,[34] J. Béquilleux,[34] A. D'Orazio,[34] M. Davier,[34] D. Derkach,[34] J. Firmino da Costa,[34] G. Grosdidier,[34] F. Le Diberder,[34] V. Lepeltier,[34] A. M. Lutz,[34] B. Malaescu,[34] S. Pruvot,[34] P. Roudeau,[34] M. H. Schune,[34] J. Serrano,[34] V. Sordini,[34,§] A. Stocchi,[34] G. Wormser,[34] D. J. Lange,[35] D. M. Wright,[35] I. Bingham,[36] J. P. Burke,[36] C. A. Chavez,[36] J. R. Fry,[36] E. Gabathuler,[36] R. Gamet,[36] D. E. Hutchcroft,[36] D. J. Payne,[36] C. Touramanis,[36] A. J. Bevan,[37] C. K. Clarke,[37] F. Di Lodovico,[37] R. Sacco,[37] M. Sigamani,[37] G. Cowan,[38] S. Paramesvaran,[38] A. C. Wren,[38] D. N. Brown,[39] C. L. Davis,[39] A. G. Denig,[40] M. Fritsch,[40] W. Gradl,[40] A. Hafner,[40] K. E. Alwyn,[41] D. Bailey,[41] R. J. Barlow,[41] G. Jackson,[41] G. D. Lafferty,[41] T. J. West,[41] J. I. Yi,[41] J. Anderson,[42] C. Chen,[42] A. Jawahery,[42] D. A. Roberts,[42] G. Simi,[42] J. M. Tuggle,[42] C. Dallapiccola,[43] E. Salvati,[43] R. Cowan,[44] D. Dujmic,[44] P. H. Fisher,[44] S. W. Henderson,[44] G. Sciolla,[44] M. Spitznagel,[44] R. K. Yamamoto,[44] M. Zhao,[44] P. M. Patel,[45] S. H. Robertson,[45] M. Schram,[45] P. Biassoni,[46a,46b] A. Lazzaro,[46a,46b] V. Lombardo,[46a] F. Palombo,[46a,46b] S. Stracka,[46a,46b] L. Cremaldi,[47] R. Godang,[47,‖] R. Kroeger,[47] P. Sonnek,[47] D. J. Summers,[47] H. W. Zhao,[47] M. Simard,[48] P. Taras,[48] H. Nicholson,[49] G. De Nardo,[50a,50b] L. Lista,[50a] D. Monorchio,[50a,50b] G. Onorato,[50a,50b] C. Sciacca,[50a,50b] G. Raven,[51] H. L. Snoek,[51] C. P. Jessop,[52] K. J. Knoepfel,[52] J. M. LoSecco,[52] W. F. Wang,[52] L. A. Corwin,[53] K. Honscheid,[53] H. Kagan,[53] R. Kass,[53] J. P. Morris,[53] A. M. Rahimi,[53] S. J. Sekula,[53] Q. K. Wong,[53] N. L. Blount,[54] J. Brau,[54] R. Frey,[54] O. Igonkina,[54] J. A. Kolb,[54] M. Lu,[54] R. Rahmat,[54] N. B. Sinev,[54] D. Strom,[54] J. Strube,[54] E. Torrence,[54] G. Castelli,[55a,55b] N. Gagliardi,[55a,55b] M. Margoni,[55a,55b] M. Morandin,[55a] M. Posocco,[55a] M. Rotondo,[55a] F. Simonetto,[55a,55b] R. Stroili,[55a,55b] C. Voci,[55a,55b] P. del Amo Sanchez,[56] E. Ben-Haim,[56] G. R. Bonneaud,[56] H. Briand,[56] J. Chauveau,[56] O. Hamon,[56] Ph. Leruste,[56] G. Marchiori,[56] J. Ocariz,[56] A. Perez,[56] J. Prendki,[56] S. Sitt,[56] L. Gladney,[57] M. Biasini,[58a,58b] E. Manoni,[58a,58b] C. Angelini,[59a,59b] G. Batignani,[59a,59b] S. Bettarini,[59a,59b] G. Calderini,[59a,59b,¶] M. Carpinelli,[59a,59b,**] A. Cervelli,[59a,59b] F. Forti,[59a,59b] M. A. Giorgi,[59a,59b] A. Lusiani,[59a,59c] M. Morganti,[59a,59b] N. Neri,[59a,59b] E. Paoloni,[59a,59b] G. Rizzo,[59a,59b] J. J. Walsh,[59a] D. Lopes Pegna,[60] C. Lu,[60] J. Olsen,[60] A. J. S. Smith,[60] A. V. Telnov,[60] F. Anulli,[61a] E. Baracchini,[61a,61b] G. Cavoto,[61a] R. Faccini,[61a,61b] F. Ferrarotto,[61a] F. Ferroni,[61a,61b] M. Gaspero,[61a,61b] P. D. Jackson,[61a] L. Li Gioi,[61a] M. A. Mazzoni,[61a] S. Morganti,[61a] G. Piredda,[61a] F. Renga,[61a,61b] C. Voena,[61a] M. Ebert,[62] T. Hartmann,[62] H. Schröder,[62] R. Waldi,[62] T. Adye,[63] B. Franek,[63] E. O. Olaiya,[63] F. F. Wilson,[63] S. Emery,[64] L. Esteve,[64] G. Hamel de Monchenault,[64] W. Kozanecki,[64] G. Vasseur,[64] Ch. Yèche,[64] M. Zito,[64] M. T. Allen,[65] D. Aston,[65] R. Bartoldus,[65] J. F. Benitez,[65] R. Cenci,[65] J. P. Coleman,[65]

M. R. Convery,[65] J. C. Dingfelder,[65] J. Dorfan,[65] G. P. Dubois-Felsmann,[65] W. Dunwoodie,[65] R. C. Field,[65] M. Franco Sevilla,[65] A. M. Gabareen,[65] M. T. Graham,[65] P. Grenier,[65] C. Hast,[65] W. R. Innes,[65] J. Kaminski,[65] M. H. Kelsey,[65] H. Kim,[65] P. Kim,[65] M. L. Kocian,[65] D. W. G. S. Leith,[65] S. Li,[65] B. Lindquist,[65] S. Luitz,[65] V. Luth,[65] H. L. Lynch,[65] D. B. MacFarlane,[65] H. Marsiske,[65] R. Messner,[65,*] D. R. Muller,[65] H. Neal,[65] S. Nelson,[65] C. P. O'Grady,[65] I. Ofte,[65] M. Perl,[65] B. N. Ratcliff,[65] A. Roodman,[65] A. A. Salnikov,[65] R. H. Schindler,[65] J. Schwiening,[65] A. Snyder,[65] D. Su,[65] M. K. Sullivan,[65] K. Suzuki,[65] S. K. Swain,[65] J. M. Thompson,[65] J. Va'vra,[65] A. P. Wagner,[65] M. Weaver,[65] C. A. West,[65] W. J. Wisniewski,[65] M. Wittgen,[65] D. H. Wright,[65] H. W. Wulsin,[65] A. K. Yarritu,[65] C. C. Young,[65] V. Ziegler,[65] X. R. Chen,[66] H. Liu,[66] W. Park,[66] M. V. Purohit,[66] R. M. White,[66] J. R. Wilson,[66] M. Bellis,[67] P. R. Burchat,[67] A. J. Edwards,[67] T. S. Miyashita,[67] S. Ahmed,[68] M. S. Alam,[68] J. A. Ernst,[68] B. Pan,[68] M. A. Saeed,[68] S. B. Zain,[68] A. Soffer,[69] S. M. Spanier,[70] B. J. Wogsland,[70] R. Eckmann,[71] J. L. Ritchie,[71] A. M. Ruland,[71] C. J. Schilling,[71] R. F. Schwitters,[71] B. C. Wray,[71] B. W. Drummond,[72] J. M. Izen,[72] X. C. Lou,[72] F. Bianchi,[73a,73b] D. Gamba,[73a,73b] M. Pelliccioni,[73a,73b] M. Bomben,[74a,74b] L. Bosisio,[74a,74b] C. Cartaro,[74a,74b] G. Della Ricca,[74a,74b] L. Lanceri,[74a,74b] L. Vitale,[74a,74b] V. Azzolini,[75] N. Lopez-March,[75] F. Martinez-Vidal,[75] D. A. Milanes,[75] A. Oyanguren,[75] J. Albert,[76] Sw. Banerjee,[76] B. Bhuyan,[76] H. H. F. Choi,[76] K. Hamano,[76] G. J. King,[76] R. Kowalewski,[76] M. J. Lewczuk,[76] I. M. Nugent,[76] J. M. Roney,[76] R. J. Sobie,[76] T. J. Gershon,[77] P. F. Harrison,[77] J. Ilic,[77] T. E. Latham,[77] G. B. Mohanty,[77] E. M. T. Puccio,[77] H. R. Band,[78] X. Chen,[78] S. Dasu,[78] K. T. Flood,[78] Y. Pan,[78] R. Prepost,[78] C. O. Vuosalo,[78] and S. L. Wu[78]

(*BABAR* Collaboration)

[1]*Laboratoire d'Annecy-le-Vieux de Physique des Particules (LAPP), Université de Savoie, CNRS/IN2P3, F-74941 Annecy-Le-Vieux, France*
[2]*Universitat de Barcelona, Facultat de Fisica, Departament ECM, E-08028 Barcelona, Spain*
[3a]*INFN Sezione di Bari, I-70126 Bari, Italy*
[3b]*Dipartimento di Fisica, Università di Bari, I-70126 Bari, Italy*
[4]*University of Bergen, Institute of Physics, N-5007 Bergen, Norway*
[5]*Lawrence Berkeley National Laboratory and University of California, Berkeley, California 94720, USA*
[6]*University of Birmingham, Birmingham, B15 2TT, United Kingdom*
[7]*Ruhr Universität Bochum, Institut für Experimentalphysik 1, D-44780 Bochum, Germany*
[8]*University of British Columbia, Vancouver, British Columbia, Canada V6T 1Z1*
[9]*Brunel University, Uxbridge, Middlesex UB8 3PH, United Kingdom*
[10]*Budker Institute of Nuclear Physics, Novosibirsk 630090, Russia*
[11]*University of California at Irvine, Irvine, California 92697, USA*
[12]*University of California at Riverside, Riverside, California 92521, USA*
[13]*University of California at San Diego, La Jolla, California 92093, USA*
[14]*University of California at Santa Barbara, Santa Barbara, California 93106, USA*
[15]*University of California at Santa Cruz, Institute for Particle Physics, Santa Cruz, California 95064, USA*
[16]*California Institute of Technology, Pasadena, California 91125, USA*
[17]*University of Cincinnati, Cincinnati, Ohio 45221, USA*
[18]*University of Colorado, Boulder, Colorado 80309, USA*
[19]*Colorado State University, Fort Collins, Colorado 80523, USA*
[20]*Technische Universität Dortmund, Fakultät Physik, D-44221 Dortmund, Germany*
[21]*Technische Universität Dresden, Institut für Kernund Teilchenphysik, D-01062 Dresden, Germany*
[22]*Laboratoire Leprince-Ringuet, CNRS/IN2P3, Ecole Polytechnique, F-91128 Palaiseau, France*
[23]*University of Edinburgh, Edinburgh EH9 3JZ, United Kingdom*
[24a]*INFN Sezione di Ferrara, I-44100 Ferrara, Italy*
[24b]*Dipartimento di Fisica, Università di Ferrara, I-44100 Ferrara, Italy*
[25]*INFN Laboratori Nazionali di Frascati, I-00044 Frascati, Italy*
[26a]*INFN Sezione di Genova, I-16146 Genova, Italy*
[26b]*Dipartimento di Fisica, Università di Genova, I-16146 Genova, Italy*
[27]*Harvard University, Cambridge, Massachusetts 02138, USA*
[28]*Universität Heidelberg, Physikalisches Institut, Philosophenweg 12, D-69120 Heidelberg, Germany*
[29]*Humboldt-Universität zu Berlin, Institut für Physik, Newtonstr. 15, D-12489 Berlin, Germany*
[30]*Imperial College London, London, SW7 2AZ, United Kingdom*
[31]*University of Iowa, Iowa City, Iowa 52242, USA*
[32]*Iowa State University, Ames, Iowa 50011-3160, USA*
[33]*Johns Hopkins University, Baltimore, Maryland 21218, USA*

[34]*Laboratoire de l'Accélérateur Linéaire, IN2P3/CNRS et Université Paris-Sud 11, Centre Scientifique d'Orsay, B. P. 34, F-91898 Orsay Cedex, France*
[35]*Lawrence Livermore National Laboratory, Livermore, California 94550, USA*
[36]*University of Liverpool, Liverpool L69 7ZE, United Kingdom*
[37]*Queen Mary, University of London, London, E1 4NS, United Kingdom*
[38]*University of London, Royal Holloway and Bedford New College, Egham, Surrey TW20 0EX, United Kingdom*
[39]*University of Louisville, Louisville, Kentucky 40292, USA*
[40]*Johannes Gutenberg-Universität Mainz, Institut für Kernphysik, D-55099 Mainz, Germany*
[41]*University of Manchester, Manchester M13 9PL, United Kingdom*
[42]*University of Maryland, College Park, Maryland 20742, USA*
[43]*University of Massachusetts, Amherst, Massachusetts 01003, USA*
[44]*Massachusetts Institute of Technology, Laboratory for Nuclear Science, Cambridge, Massachusetts 02139, USA*
[45]*McGill University, Montréal, Québec, Canada H3A 2T8*
[46a]*INFN Sezione di Milano, I-20133 Milano, Italy*
[46b]*Dipartimento di Fisica, Università di Milano, I-20133 Milano, Italy*
[47]*University of Mississippi, University, Mississippi 38677, USA*
[48]*Université de Montréal, Physique des Particules, Montréal, Québec, Canada H3C 3J7*
[49]*Mount Holyoke College, South Hadley, Massachusetts 01075, USA*
[50a]*INFN Sezione di Napoli, I-80126 Napoli, Italy*
[50b]*Dipartimento di Scienze Fisiche, Università di Napoli Federico II, I-80126 Napoli, Italy*
[51]*NIKHEF, National Institute for Nuclear Physics and High Energy Physics, NL-1009 DB Amsterdam, The Netherlands*
[52]*University of Notre Dame, Notre Dame, Indiana 46556, USA*
[53]*Ohio State University, Columbus, Ohio 43210, USA*
[54]*University of Oregon, Eugene, Oregon 97403, USA*
[55a]*INFN Sezione di Padova, I-35131 Padova, Italy*
[55b]*Dipartimento di Fisica, Università di Padova, I-35131 Padova, Italy*
[56]*Laboratoire de Physique Nucléaire et de Hautes Energies, IN2P3/CNRS, Université Pierre et Marie Curie-Paris6, Université Denis Diderot-Paris7, F-75252 Paris, France*
[57]*University of Pennsylvania, Philadelphia, Pennsylvania 19104, USA*
[58a]*INFN Sezione di Perugia, I-06100 Perugia, Italy*
[58b]*Dipartimento di Fisica, Università di Perugia, I-06100 Perugia, Italy*
[59a]*INFN Sezione di Pisa, I-56127 Pisa, Italy*
[59b]*Dipartimento di Fisica, Università di Pisa, I-56127 Pisa, Italy*
[59c]*Scuola Normale Superiore di Pisa, I-56127 Pisa, Italy*
[60]*Princeton University, Princeton, New Jersey 08544, USA*
[61a]*INFN Sezione di Roma, I-00185 Roma, Italy*
[61b]*Dipartimento di Fisica, Università di Roma La Sapienza, I-00185 Roma, Italy*
[62]*Universität Rostock, D-18051 Rostock, Germany*
[63]*Rutherford Appleton Laboratory, Chilton, Didcot, Oxon, OX11 0QX, United Kingdom*
[64]*CEA, Irfu, SPP, Centre de Saclay, F-91191 Gif-sur-Yvette, France*
[65]*SLAC National Accelerator Laboratory, Stanford, California 94309 USA*
[66]*University of South Carolina, Columbia, South Carolina 29208, USA*
[67]*Stanford University, Stanford, California 94305-4060, USA*
[68]*State University of New York, Albany, New York 12222, USA*
[69]*Tel Aviv University, School of Physics and Astronomy, Tel Aviv, 69978, Israel*
[70]*University of Tennessee, Knoxville, Tennessee 37996, USA*
[71]*University of Texas at Austin, Austin, Texas 78712, USA*
[72]*University of Texas at Dallas, Richardson, Texas 75083, USA*
[73a]*INFN Sezione di Torino, I-10125 Torino, Italy*
[73b]*Dipartimento di Fisica Sperimentale, Università di Torino, I-10125 Torino, Italy*
[74a]*INFN Sezione di Trieste, I-34127 Trieste, Italy*

[*]Deceased
[†]Now at Temple University, Philadelphia, PA 19122, USA.
[‡]Also at Università di Perugia, Dipartimento di Fisica, Perugia, Italy.
[§]Also at Università di Roma La Sapienza, I-00185 Roma, Italy.
[‖]Now at University of South Alabama, Mobile, AL 36688, USA.
[¶]Also at Laboratoire de Physique Nucléaire et de Hautes Energies, IN2P3/CNRS, Université Pierre et Marie Curie-Paris6, Université Denis Diderot-Paris7, F-75252 Paris, France.
[**]Also at Università di Sassari, Sassari, Italy.

[74b]*Dipartimento di Fisica, Università di Trieste, I-34127 Trieste, Italy*
[75]*IFIC, Universitat de Valencia-CSIC, E-46071 Valencia, Spain*
[76]*University of Victoria, Victoria, British Columbia, Canada V8W 3P6*
[77]*Department of Physics, University of Warwick, Coventry CV4 7AL, United Kingdom*
[78]*University of Wisconsin, Madison, Wisconsin 53706, USA*

(Received 13 July 2009; revised manuscript received 9 November 2009; published 9 December 2009)

We present updated measurements of the branching fractions for B^0 meson decays to ηK^0, $\eta\eta$, $\eta\phi$, $\eta\omega$, $\eta' K^0$, $\eta'\eta'$, $\eta'\phi$, and $\eta'\omega$, and branching fractions and *CP*-violating charge asymmetries for B^+ decays to $\eta\pi^+$, ηK^+, $\eta'\pi^+$, and $\eta' K^+$. The data represent the full data set of 467×10^6 $B\bar{B}$ pairs collected with the *BABAR* detector at the PEP-II asymmetric-energy e^+e^- collider at the SLAC National Accelerator Laboratory. Besides large signals for the four charged B decay modes and for $B^0 \to \eta' K^0$, we find evidence for three B^0 decay modes at greater than 3.0σ significance. We find $\mathcal{B}(B^0 \to \eta K^0) = (1.15^{+0.43}_{-0.38} \pm 0.09) \times 10^{-6}$, $\mathcal{B}(B^0 \to \eta\omega) = (0.94^{+0.35}_{-0.30} \pm 0.09) \times 10^{-6}$, and $\mathcal{B}(B^0 \to \eta'\omega) = (1.01^{+0.46}_{-0.38} \pm 0.09) \times 10^{-6}$, where the first (second) uncertainty is statistical (systematic). For the $B^+ \to \eta K^+$ decay mode, we measure the charge asymmetry $\mathcal{A}_{\rm ch}(B^+ \to \eta K^+) = -0.36 \pm 0.11 \pm 0.03$.

DOI: 10.1103/PhysRevD.80.112002 PACS numbers: 13.25.Hw, 11.30.Er, 12.15.Hh

Experimental measurements of branching fractions and *CP*-violating charge asymmetries in rare B decays play an important role in testing the theoretical predictions of the standard model and its extensions. We report the results of branching fraction measurements for B^0 meson decays to ηK^0, $\eta\eta$, $\eta\phi$, $\eta\omega$, $\eta' K^0$, $\eta'\eta'$, $\eta'\phi$, and $\eta'\omega$ final states and of branching fraction and charge asymmetry measurements for B^+ decays to $\eta\pi^+$, ηK^+, $\eta'\pi^+$, and $\eta' K^+$ [1]. We search for charge asymmetry by measuring

$$\mathcal{A}_{\rm ch} \equiv \frac{\Gamma^- - \Gamma^+}{\Gamma^- + \Gamma^+}, \tag{1}$$

where $\Gamma^\pm = \Gamma(B^\pm \to f^\pm)$ is the decay width for a given charged final state $f^\pm$. These branching fraction and charge asymmetry measurements represent an improvement over previous results published by *BABAR* [2] and Belle [3].

The branching fractions and charge asymmetries of the charmless hadronic B decays are predicted using approaches based on QCD factorization [4–7] and flavor SU(3) symmetry [8–10]. These B decays proceed through loop (penguin) and suppressed tree diagram amplitudes, as shown in Fig. 1. The branching fraction and charge asymmetry measurements may provide sensitivity to the presence of heavy nonstandard model particles in the loop diagrams [11]. The measured $\eta' K$ branching fraction is found to be much larger than the ηK one [2,3]. Many suggestions have been proposed to explain such a difference, including flavor singlet enhancement [12], intrinsic charm [13], and constructively interfering internal penguin diagrams [14,15]. This last approach is supported by next-to-leading order QCD factorization calculations [6].

The *CP*-violating parameters $S_{\eta' K}$ and $S_{\phi K}$, measured in the time-dependent analysis of $\eta' K^0$ and ϕK^0 decays [16], are expected to equal $S_{c\bar{c}s} \approx \sin 2\beta$, where $S_{c\bar{c}s}$ is measured in the Cabibbo-Kobayashi-Maskawa (CKM) favored $b \to c\bar{c}s$ decays, if penguin $b \to s$ transitions are dominant. However, CKM-suppressed amplitudes and color-suppressed tree diagrams can introduce additional weak phases whose contributions may not be negligible [6,17,18]. As a consequence, deviations from $\sin 2\beta$ may occur even within the standard model. Rates of the decay modes to $\eta\eta$, $\eta\phi$, $\eta'\eta'$, and $\eta'\phi$ are used in flavor SU(3)-based calculations of the $|S_{c\bar{c}s} - S_f|$ (with $f = \eta' K$, ϕK) bound [17]. This bound may be improved by more precise measurements of the branching fractions of these modes.

The charge asymmetry is expected to be sizable in ηK^+ and suppressed in $\eta' K^+$ decays [6,9,19]. However, different approaches predict the two asymmetries to have the same [9] or opposite [6] signs; precise measurement of such asymmetries can discriminate between these models. Furthermore, the charge asymmetries in $\eta'\pi^+$ and $\eta\pi^+$ decays are expected to be sizable [6,9], with model-dependent predictions for their magnitudes.

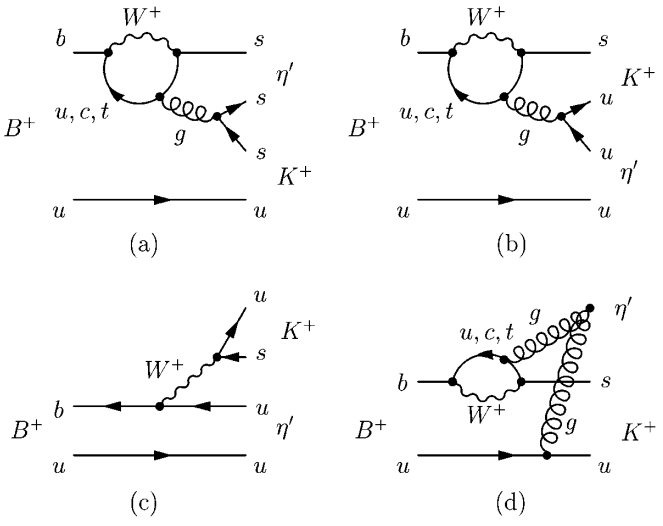

FIG. 1. Examples of Feynman diagrams involved in decays studied in this paper: (a), (b) penguin diagrams, (c) Cabibbo-suppressed tree diagram, (d) gluonic penguin diagram.

The results presented here are based on the full data set collected with the *BABAR* detector [20] at the PEP-II asymmetric-energy e^+e^- collider located at the SLAC National Accelerator Laboratory. An integrated luminosity of 426 fb^{-1}, corresponding to $N_{B\bar{B}} = 467 \times 10^6$ $B\bar{B}$ pairs, was recorded at the $\Upsilon(4S)$ resonance (center-of-mass energy $\sqrt{s} = 10.58$ GeV). A further 44 fb^{-1} was collected approximately 40 MeV below the resonance (off-peak) for the study of the $e^+e^- \to q\bar{q}$ background, where q is a u, d, s, or c quark.

Charged particles are detected, and their momenta measured, by a combination of a vertex tracker, consisting of five layers of double-sided silicon microstrip detectors, and a 40-layer drift chamber, both operating in the 1.5 T magnetic field of a superconducting solenoid. We identify photons and electrons using a CsI(Tl) electromagnetic calorimeter (EMC). Further charged-particle identification (PID) is provided by the average energy loss ($\mathrm{d}E/\mathrm{d}x$) measurements in the tracking devices and by the information provided by an internally reflecting ring-imaging Cherenkov detector (DIRC) covering the central region.

We select η, η', ϕ, ρ^0, K^0_S, ω, and π^0 candidates through the decays $\eta \to \gamma\gamma$ ($\eta_{\gamma\gamma}$), $\eta \to \pi^+\pi^-\pi^0$ ($\eta_{3\pi}$), $\eta' \to \eta\pi^+\pi^-$ with $\eta \to \gamma\gamma$ ($\eta'_{\eta\pi\pi}$), $\eta' \to \rho^0\gamma$ ($\eta'_{\rho\gamma}$), $\phi \to K^+K^-$, $\rho^0 \to \pi^+\pi^-$, $K^0_S \to \pi^+\pi^-$, $\omega \to \pi^+\pi^-\pi^0$, and $\pi^0 \to \gamma\gamma$. We do not study the decay $B^0 \to \eta'\eta'$ with both η' mesons decaying to $\rho\gamma$, because it suffers large backgrounds. Requirements applied to the photon energy E_γ and to the invariant mass of the B daughters are listed in Table I. The requirements on the η and η' invariant masses depend on the decay mode. Branching fractions of charged B decays with η' in the final state and of $B^0 \to \eta' K^0_S$ are higher than those of the other neutral B modes. In neutral decay modes we apply a tighter requirement on $\eta_{3\pi}$ invariant mass in order to prevent possible contamination from $B\bar{B}$ background. The different requirements on the η' mass increase the purity of the charged B and $\eta' K^0_S$ modes and enhance the selection efficiency for the other neutral B decay modes. The energy (momentum) of the π^0 (η) candidates is required to exceed 200 MeV (200 MeV/c) in the laboratory frame. The prompt charged tracks in $B^+ \to \eta'\pi^+$ and secondary charged tracks in η, η', and ω candidates are required to have DIRC, $\mathrm{d}E/\mathrm{d}x$, and EMC signatures consistent with the pion hypothesis. After selection, we constrain the η, η', and π^0 masses to their world average values [21]. The prompt charged track in $B^+ \to \eta' K^+$ is required to be consistent with the kaon hypothesis. The signatures for the charged kaons from ϕ decays are required to be inconsistent with hypotheses for electrons, pions and protons. For the prompt charged track in B^+ decays to ηK^+ and $\eta\pi^+$, we define the variables $\mathcal{C}_K$ and $\mathcal{C}_\pi$ as

$$\mathcal{C}_{K,\pi} = \frac{\theta^{\mathrm{meas}}_{K,\pi} - \theta^{\mathrm{exp}}_{K,\pi}}{\sigma^{\mathrm{meas}}_{K,\pi}}, \tag{2}$$

where $\theta^{\mathrm{meas}}_{K,\pi}$ ($\theta^{\mathrm{exp}}_{K,\pi}$) is the measured (expected) DIRC Cherenkov angle and $\sigma^{\mathrm{meas}}_{K,\pi}$ is its uncertainty, for the kaon and pion hypothesis, respectively. We require $-3 < \mathcal{C}_K < 13$ and $-13 < \mathcal{C}_\pi < 3$. For K^0_S candidates we require a vertex χ^2 probability larger than 0.001 and a reconstructed decay length greater than 3 times its uncertainty.

We reconstruct the B meson candidate by combining the four-momenta of the final state particles and imposing a vertex constraint. A B meson candidate is kinematically characterized by the energy-substituted mass $m_{\mathrm{ES}} = \sqrt{s/4 - \mathbf{p}^2_B}$ and energy difference $\Delta E = E_B - \frac{1}{2}\sqrt{s}$, where $(E_B, \mathbf{p}_B)$ is the B-meson four-momentum vector expressed

TABLE I. Selection requirements on the invariant masses of the signal resonances and on the laboratory energies of the photons coming from their decays.

State	Invariant mass (MeV/c^2)	E_γ (MeV)
π^0	$120 < m_{\gamma\gamma} < 150$	>30
Prompt $\eta_{\gamma\gamma}$	$505 < m_{\gamma\gamma} < 585$	>100
Secondary $\eta_{\gamma\gamma}$	$490 < m_{\gamma\gamma} < 600$	>50[a]
$\eta_{3\pi}$ in B^+ decays	$534 < m_{\pi\pi\pi} < 561$	...
$\eta_{3\pi}$ in B^0 decays	$535 < m_{\pi\pi\pi} < 555$	...
$\eta'_{\eta\pi\pi}$ in B^+ and $B^0 \to \eta' K^0_S$ decays	$945 < m_{\eta\pi\pi} < 970$	...
$\eta'_{\eta\pi\pi}$ in other B^0 decays	$930 < m_{\eta\pi\pi} < 990$	...
$\eta'_{\rho\gamma}$ in B^+ decays	$930 < m_{\rho\gamma} < 980$	>200
$\eta'_{\rho\gamma}$ in $B^0 \to \eta'_{\rho\gamma} K^0_S$	$930 < m_{\rho\gamma} < 980$	>100
$\eta'_{\rho\gamma}$ in other B^0 decays	$910 < m_{\rho\gamma} < 990$	>200
ρ^0	$470 < m_{\pi\pi} < 990$	...
ω	$735 < m_{\pi\pi\pi} < 825$	...
ϕ	$1012 < m_{K^+K^-} < 1026$	...
K^0_S	$486 < m_{\pi\pi} < 510$	...

[a] $E_\gamma > 100$ MeV in the $B^+ \to \eta'_{\eta\pi\pi} K^+$ and $B^+ \to \eta'_{\eta\pi\pi}\pi^+$ decay modes.

in the $\Upsilon(4S)$ rest frame. For signal events, the $m_{\rm ES}$ and ΔE distributions peak around 5.28 GeV/c^2 and zero, respectively. We require $5.25 < m_{\rm ES} < 5.29$ GeV/c^2 and $|\Delta E| < 0.2$ GeV for all decay modes except $B^0 \to \eta K^0_S$, where we require $-0.15 < \Delta E < 0.2$ GeV in order to suppress most of the background from radiative B decays.

Backgrounds arise primarily from random combinations of tracks and neutral clusters in $e^+e^- \to q\bar{q}$ continuum events. We use large samples of Monte Carlo (MC) simulated [22] events and control samples to optimize criteria to suppress the background. We reject continuum events by using the angle $\theta_{\rm T}$ between the thrust axis of the B candidate in the $\Upsilon(4S)$ frame and that of the rest of the event. The thrust axis of the B candidate is given by the thrust axis of the B decay products. The distribution of $|\cos\theta_{\rm T}|$ is sharply peaked near 1.0 for jetlike $q\bar{q}$ pair events and is nearly uniform for $\Upsilon(4S) \to B\bar{B}$ events. We require $|\cos\theta_{\rm T}| < 0.9$ (0.85 for $\eta'_{\rho\gamma}\pi^+$, 0.8 for $\eta_{\gamma\gamma}\omega$ and $\eta'_{\rho\gamma}\omega$). To discriminate against τ-pair and two-photon backgrounds, and to better describe the event shape, we require the event to contain at least three charged tracks, or one track beyond the minimum required for the signal decay topology, whichever is larger.

In $\eta \to \gamma\gamma$ (ϕ) decays, we define $\mathcal{H}_\eta$ ($\mathcal{H}_\phi$) as the cosine of the angle between the direction of a daughter γ (K) and the flight direction of the parent of η (ϕ) in the η (ϕ) rest frame; for $\eta'_{\rho\gamma}$, $\mathcal{H}_\rho$ is the cosine of the angle between the direction of a daughter pion and the flight direction of the η' in the ρ rest frame. For B decays containing an ω meson in the final state we define $\mathcal{H}_\omega$ as the cosine of the angle between the B recoil direction and the normal to the plane defined by the ω daughters in the ω rest frame. We require $|\mathcal{H}_\eta| < 0.95$ in $B^0 \to \eta\eta$ decay modes. We reject candidate events if $|\mathcal{H}_\rho| > 0.9$ (> 0.75 in the $B^+ \to \eta'_{\rho\gamma}\pi^+$ decay mode).

For the $B^0 \to \eta_{\gamma\gamma}K^0_S$ ($B^+ \to \eta_{\gamma\gamma}h^+$, $h^+ = K^+$, π^+) decay, the main source of $B\bar{B}$ background is the $B^0 \to \pi^0 K^0_S$ ($B^+ \to \pi^0 h^+$) decay. To suppress this background, we search for π^0 candidates with a photon in common (overlapping) with the η candidate from the reconstructed signal B candidate. We require the π^0 mass not to be in the range $(0.117, 0.152)$ GeV/c^2 for the $B^0 \to \eta_{\gamma\gamma}K^0_S$ decay mode, and $(0.118, 0.150)$ GeV/c^2 for the $B^+ \to \eta_{\gamma\gamma}h^+$ decay modes. Further suppression of this background is obtained with suitable requirements on $|\mathcal{H}_\eta|$ and on the energy of the second (nonoverlapping with η) π^0 photon ($E^{\rm 2nd}_\gamma$). We optimize these requirements by maximizing $S/\sqrt{S+B}$, where S (B) is the number of signal (background) events surviving the selection. We find the optimal criteria to be $|\mathcal{H}_\eta| < 0.966$ and $E^{\rm 2nd}_\gamma < 0.207$ GeV for the $B^0 \to \eta_{\gamma\gamma}K^0_S$ decay mode, and $|\mathcal{H}_\eta| < 0.977$ and $E^{\rm 2nd}_\gamma < 0.143$ GeV for the $B^+ \to \eta_{\gamma\gamma}h^+$ decay modes.

We find a mean number of B candidates per event in the range 1.0–1.4, depending on the final state. Signal events are divided into two categories: a correctly reconstructed (CR) signal where all candidate particles come from the correct signal B, and a self cross-feed (SCF) signal where at least one candidate particle is exchanged with a particle coming from the rest of the event. Simulations show that the fraction of SCF candidates is in the range (3–7)% in charged B decay modes and (2–20)% in neutral B decay modes. If an event has multiple B candidates, we select the candidate with the highest B vertex χ^2 probability, determined from a vertex fit that includes both charged and neutral particles [23]. This algorithm selects the correct candidate, if present, with an efficiency of (91–99)% and introduces negligible bias.

We obtain yields from unbinned extended maximum-likelihood (ML) fits. The main input observables are ΔE, $m_{\rm ES}$, and a Fisher discriminant $\mathcal{F}$ [24]. Where relevant, the invariant masses $m_{\rm res}$ of the intermediate resonances and angular variables $\mathcal{H}$ are used. The Fisher discriminant $\mathcal{F}$ combines five variables: the angles with respect to the beam axis of the B momentum and B thrust axis, the zeroth and second angular moments $L_{0,2}$ of the energy flow about the B thrust axis, and the absolute value of the continuous output of a flavor-tagging algorithm. The first four variables are evaluated in the $\Upsilon(4S)$ rest frame. The moments are defined by $L_r = \sum_s p_s \times |\cos\theta_s|^r$, where θ_s is the angle with respect to the B thrust axis of track or neutral cluster s with momentum p_s, and the sum excludes the B candidate. Flavor-tagging information is derived from an analysis of the decay products of the non-signal candidate B meson ($B_{\rm tag}$), using a neural network based technique [25]. The output value of the tagging algorithm reflects the different final states identified in $B_{\rm tag}$ decay. In particular, the presence of a lepton in the final state usually results in a large tagging output value, for both $B^0\bar{B}^0$ and B^+B^- events. Since leptons are not generally present in continuum background events, the inclusion of the tagging algorithm output in $\mathcal{F}$ improves its discriminating power between continuum background and $B\bar{B}$ events. The coefficients of $\mathcal{F}$ are chosen to maximize the separation between the signal and the continuum background. They are determined from studies of MC signal events and off-peak data.

The set of probability density functions (PDF) used in the ML fits, specific to each decay mode, is determined on the basis of studies with MC samples. We estimate $B\bar{B}$ backgrounds using MC samples of B decays. Where needed, we add components to account for $B\bar{B}$ background events with a $m_{\rm ES}$ or ΔE distribution that peaks in the signal region and for background from B meson decays with charmed particles in the final state.

The extended likelihood function is

$$\mathcal{L} = \exp\Big(-\sum_{j=1}^{3} n_j\Big)\prod_{i=1}^{N}\Big[\sum_{j=1}^{3} n_j \mathcal{P}_j(\mathbf{x}_i)\Big], \qquad (3)$$

where N is the number of input events, n_j is the number of events for hypothesis j ($j = 1$ for signal, $j = 2$ for continuum background, and $j = 3$ for $B\bar{B}$ background), and $\mathcal{P}_j(\mathbf{x}_i)$ is the corresponding PDF evaluated with the observables $\mathbf{x}_i$ of the ith event. In the $B^0 \to \eta'\omega$, $\eta'\phi$, and $\eta'_{\rho\gamma}\omega$ decay modes the signal includes both the CR and SCF signal components with the SCF fraction fixed to the value estimated from simulation. Because of the similar kinematics and branching fractions of the ηK^+ and $\eta\pi^+$ decay modes, we perform a combined fit to extract the two signal yields and charge asymmetries. In this fit we use the $\mathcal{C}_K$ and $\mathcal{C}_\pi$ variables to discriminate the mass hypothesis of the prompt track. Since the correlations among the observables in the data are small, we assume each $\mathcal{P}_j$ to be the product of the PDFs for the separate variables. Correlations between the ηK^+ and $\eta\pi^+$ signal yields (charge asymmetries) are below 5% (7%).

We determine the PDF functional form and parameters from MC simulation for the signal and $B\bar{B}$ backgrounds, and from sideband data ($5.25 < m_{\rm ES} < 5.27$ GeV/c^2; $0.1 < |\Delta E| < 0.2$ GeV) for the continuum background. For $B^+ \to \eta h^+$ decay modes, PDF functional form and parameters for the continuum background are determined using off-peak data. We parameterize each of the functions $\mathcal{P}_1(m_{\rm ES})$, $\mathcal{P}_1(\Delta E)$, $\mathcal{P}_j(\mathcal{F})$, and the peaking components of $\mathcal{P}_j(m_{\rm res})$ with either a symmetric or a bifurcated Gaussian, the sum of two symmetric or bifurcated Gaussian shapes, a bifurcated Gaussian distribution with exponential tails [26] or a Crystal Ball function [27], as required to describe the distribution. Slowly varying distributions ($m_{\rm res}$ and ΔE for the continuum background, and angular variables) are represented by linear or quadratic functions. For the continuum background, the $m_{\rm ES}$ distribution is described by the ARGUS function [28]. Large data control samples of B decays to charmed final states of similar topologies are used to verify the simulated resolutions in $m_{\rm ES}$ and ΔE. Where the control samples reveal differences between data and MC samples in mass (energy) resolution, we correct the mean and scale the width of the mass (energy) distribution used in the likelihood fits.

The validity of the fit procedure and PDF parameterization, including the effects of unmodeled correlations among observables, is checked with simulated experiments. This is done by embedding a number of signal and peaking $B\bar{B}$ background events from fully simulated MC samples and by drawing a number of $q\bar{q}$ and charm $B\bar{B}$ events from PDFs, according to the values found in the data. In each fit the free parameters are the yields, the charge asymmetry for the signal and continuum background, and several parameters describing the ΔE, $m_{\rm ES}$, and $\mathcal{F}$ distributions of the continuum background. A systematic uncertainty due to fixing signal and background parameters in the fit is accounted. The charge asymmetry for $B\bar{B}$ background is fixed to zero in the fit. A systematic is evaluated to account for this restriction.

Tables II and III show, for B^0 and B^+ decays, respectively, the measured yields, fit biases, efficiencies, and products of daughter branching fractions for each decay mode. The efficiency is calculated as the ratio of the number of signal MC events after the event selection to the total generated, and is corrected for known differences between simulations and data. We compute the branching fractions from the fitted signal event yields, reconstruction efficiencies, daughter branching fractions, and the number of produced B mesons $N_{B\bar{B}}$, assuming equal production rates of charged and neutral B pairs from $\Upsilon(4S)$ decays. We correct the yields for any bias measured with the simulations. We combine results from different subdecays by adding the values of $-2\ln(\mathcal{L}/\mathcal{L}_{\rm max})$ (parameterized in terms of the branching fraction or charge asymmetry), where $\mathcal{L}_{\rm max}$ is the value of $\mathcal{L}$ at its maximum, taking into account the correlated and uncorrelated systematic errors. We report the branching fractions for the individual decay channels and their significances $\mathcal{S}$ in units of standard deviations (σ). For $B^0 \to \eta' K^0_S$ and all charged decay modes, where the significance of the branching fraction is always greater than 7σ, the value of $\mathcal{S}$ is omitted. For the combined measurements we also report the 90% confidence level (CL) upper limits of the branching fraction for the B^0 modes where the significance is less than 5σ. For charged B decays we give the combined result for the charge asymmetry $\mathcal{A}_{\rm ch}$ and its significance $\mathcal{S}_{\mathcal{A}}$ in units of σ.

The statistical uncertainty on the signal yield and charge asymmetry is calculated as the change in the central value when the quantity $-2\ln\mathcal{L}$ increases by one from its minimum. The significance is calculated as the square root of $-2\ln(\mathcal{L}_0/\mathcal{L}_{\rm max})$, with systematic uncertainties included, where $\mathcal{L}_0$ is the value of $\mathcal{L}$ for zero signal events or zero value for the charge asymmetry. We determine a Bayesian 90% CL upper limit on the branching fraction, assuming a uniform prior probability distribution, by finding the branching fraction below which lies 90% of the total of the likelihood integral in the positive branching fraction region.

Figures 2 and 3 show the projections onto the $m_{\rm ES}$ and ΔE variables for the four neutral decay modes that have a branching fraction significance greater than 3σ, and for the four charged decay modes, respectively. For each decay mode we optimize a requirement on the probability ratio $\mathcal{P}_1/(\mathcal{P}_1 + \mathcal{P}_2 + \mathcal{P}_3)$ in order to enhance the visibility of the signal. The probabilities $\mathcal{P}_j$ are evaluated without using the variable shown. The points show the data that satisfy such a requirement, while the solid curves show the total rescaled fit functions. In $\eta'\omega$ decays, a fit performed on ω mass sidebands $m_{\pi\pi\pi} < 735$ MeV/c^2 or $m_{\pi\pi\pi} > 825$ MeV/c^2 shows that contamination from possible $B^0 \to \eta'\pi^+\pi^-\pi^0$ background is negligible.

The main sources of systematic error include ML fit bias (0–14 events) and uncertainties in the PDF parameteriza-

TABLE II. Fitted signal event yield and fit bias in events (ev), detection efficiency ϵ, daughter branching fraction product $\prod \mathcal{B}_i$, significance $\mathcal{S}$, and measured branching fraction $\mathcal{B}$ with statistical error for each B^0 decay mode. For the combined measurements we give the significance (with systematic uncertainties included) and the branching fraction with the statistical and systematic uncertainties (in parentheses the 90% CL upper limit). Significances greater than 7 standard deviations (σ) are omitted.

Mode	Yield (ev)	Fit bias (ev)	ϵ (%)	$\prod \mathcal{B}_i$ (%)	$\mathcal{S}(\sigma)$	$\mathcal{B}(10^{-6})$	
$\eta_{\gamma\gamma}K^0$	21^{+10}_{-9}	0	32.1	13.6	2.5	$1.03^{+0.49}_{-0.44}$	
$\eta_{3\pi}K^0$	12^{+7}_{-6}	0	20.6	7.9	2.5	$1.56^{+0.92}_{-0.79}$	
$\boldsymbol{\eta K^0}$					**3.5**	$\mathbf{1.15^{+0.43}_{-0.38} \pm 0.09}$	$(<\mathbf{1.8})$
$\eta_{\gamma\gamma}\eta_{\gamma\gamma}$	13^{+10}_{-9}	+1	23.9	15.5	1.4	$0.7^{+0.6}_{-0.5}$	
$\eta_{\gamma\gamma}\eta_{3\pi}$	9^{+6}_{-5}	+1	18.0	17.9	1.5	$0.5^{+0.4}_{-0.3}$	
$\eta_{3\pi}\eta_{3\pi}$	$0.2^{+2.4}_{-1.7}$	−0.1	11.1	5.2	0.1	$0.1^{+0.9}_{-0.6}$	
$\boldsymbol{\eta\eta}$					**1.9**	$\mathbf{0.5 \pm 0.3 \pm 0.1}$	$(<\mathbf{1.0})$
$\eta_{\gamma\gamma}\phi$	0^{+6}_{-5}	0	29.3	19.4	0.1	0.0 ± 0.2	
$\eta_{3\pi}\phi$	4^{+4}_{-3}	0	18.3	11.2	1.9	$0.4^{+0.4}_{-0.3}$	
$\boldsymbol{\eta\phi}$					**1.4**	$\mathbf{0.2 \pm 0.2 \pm 0.1}$	$(<\mathbf{0.5})$
$\eta_{\gamma\gamma}\omega$	36^{+13}_{-12}	+3	18.7	35.1	3.4	$1.08^{+0.42}_{-0.39}$	
$\eta_{3\pi}\omega$	8^{+7}_{-5}	+1	13.1	20.2	1.8	$0.59^{+0.57}_{-0.40}$	
$\boldsymbol{\eta\omega}$					**3.7**	$\mathbf{0.94^{+0.35}_{-0.30} \pm 0.09}$	$(<\mathbf{1.4})$
$\eta'_{\eta\pi\pi}K^0$	490^{+25}_{-24}	−2	26.6	6.1	⋯	$64.9^{+3.3}_{-3.2}$	
$\eta'_{\rho\gamma}K^0$	1003 ± 41	+27	28.3	10.2	⋯	72.4 ± 3.0	
$\boldsymbol{\eta' K^0}$					⋯	$\mathbf{68.5 \pm 2.2 \pm 3.1}$	
$\eta'_{\eta\pi\pi}\eta'_{\eta\pi\pi}$	$1.6^{+2.1}_{-1.1}$	0	19.9	3.1	2.2	$0.6^{+0.7}_{-0.3}$	
$\eta'_{\eta\pi\pi}\eta'_{\rho\gamma}$	8^{+9}_{-7}	+2	19.8	10.3	0.8	$0.6^{+0.9}_{-0.7}$	
$\boldsymbol{\eta'\eta'}$					**1.0**	$\mathbf{0.6^{+0.5}_{-0.4} \pm 0.4}$	$(<\mathbf{1.7})$
$\eta'_{\eta\pi\pi}\phi$	-2^{+2}_{-1}	0	24.4	8.6	0.0	$-0.2^{+0.2}_{-0.1}$	
$\eta'_{\rho\gamma}\phi$	5^{+8}_{-7}	0	23.9	14.5	0.7	$0.3^{+0.5}_{-0.4}$	
$\boldsymbol{\eta'\phi}$					**0.5**	$\mathbf{0.2 \pm 0.2 \pm 0.3}$	$(<\mathbf{1.1})$
$\eta'_{\eta\pi\pi}\omega$	14^{+7}_{-6}	+1	17.9	15.6	3.4	$1.03^{+0.54}_{-0.46}$	
$\eta'_{\rho\gamma}\omega$	16^{+17}_{-15}	−2	15.2	26.2	1.2	$0.94^{+0.91}_{-0.81}$	
$\boldsymbol{\eta'\omega}$					**3.6**	$\mathbf{1.01^{+0.46}_{-0.38} \pm 0.09}$	$(<\mathbf{1.8})$

TABLE III. Fitted signal event yield and fit bias in events (ev), detection efficiency ϵ, daughter branching fraction product $\prod \mathcal{B}_i$, measured branching fraction $\mathcal{B}$, charge asymmetry $\mathcal{A}_{\rm ch}$ with statistical error, and significance $\mathcal{S}_{\mathcal{A}}$ of the charge asymmetry for each charged decay mode. For the combined measurements we give the branching fraction, the charge asymmetry and the significance of the charge asymmetry with the statistical and systematic uncertainties.

Mode	Yield (ev)	Fit bias (ev)	ϵ (%)	$\prod \mathcal{B}_i$ (%)	$\mathcal{B}(10^{-6})$	$\mathcal{A}_{\rm ch}$	$\mathcal{S}_{\mathcal{A}}(\sigma)$
$\eta_{\gamma\gamma}\pi^+$	286^{+31}_{-30}	+18	35.1	39.3	$4.16^{+0.48}_{-0.47}$	$-0.02^{+0.10}_{-0.11}$	0.4
$\eta_{3\pi}\pi^+$	95^{+19}_{-18}	+7	23.4	22.7	$3.53^{+0.77}_{-0.73}$	$+0.06 \pm 0.18$	0.4
$\boldsymbol{\eta\pi^+}$					$\mathbf{4.00 \pm 0.40 \pm 0.24}$	$\mathbf{-0.03 \pm 0.09 \pm 0.03}$	**0.3**
$\eta_{\gamma\gamma}K^+$	215^{+31}_{-30}	+21	34.0	39.3	$3.11^{+0.50}_{-0.48}$	-0.37 ± 0.12	3.1
$\eta_{3\pi}K^+$	69^{+16}_{-15}	+6	22.9	22.7	$2.60^{+0.66}_{-0.62}$	-0.32 ± 0.22	1.5
$\boldsymbol{\eta K^+}$					$\mathbf{2.94^{+0.39}_{-0.34} \pm 0.21}$	$\mathbf{-0.36 \pm 0.11 \pm 0.03}$	**3.3**
$\eta'_{\eta\pi\pi}\pi^+$	96^{+20}_{-19}	+1	29.4	17.5	4.0 ± 0.8	-0.25 ± 0.19	1.3
$\eta'_{\rho\gamma}\pi^+$	111^{+31}_{-29}	+7	25.9	29.4	$2.9^{+0.9}_{-0.8}$	$+0.56^{+0.29}_{-0.27}$	2.1
$\boldsymbol{\eta'\pi^+}$					$\mathbf{3.5 \pm 0.6 \pm 0.2}$	$\mathbf{+0.03 \pm 0.17 \pm 0.02}$	**0.2**
$\eta'_{\eta\pi\pi}K^+$	1601^{+44}_{-43}	−5	28.7	17.5	$68.5^{+1.9}_{-1.8}$	-0.004 ± 0.027	0.2
$\eta'_{\rho\gamma}K^+$	2991^{+72}_{-71}	−10	29.3	29.4	74.6 ± 1.8	$+0.016 \pm 0.023$	0.7
$\boldsymbol{\eta' K^+}$					$\mathbf{71.5 \pm 1.3 \pm 3.2}$	$\mathbf{+0.008^{+0.017}_{-0.018} \pm 0.009}$	**0.4**

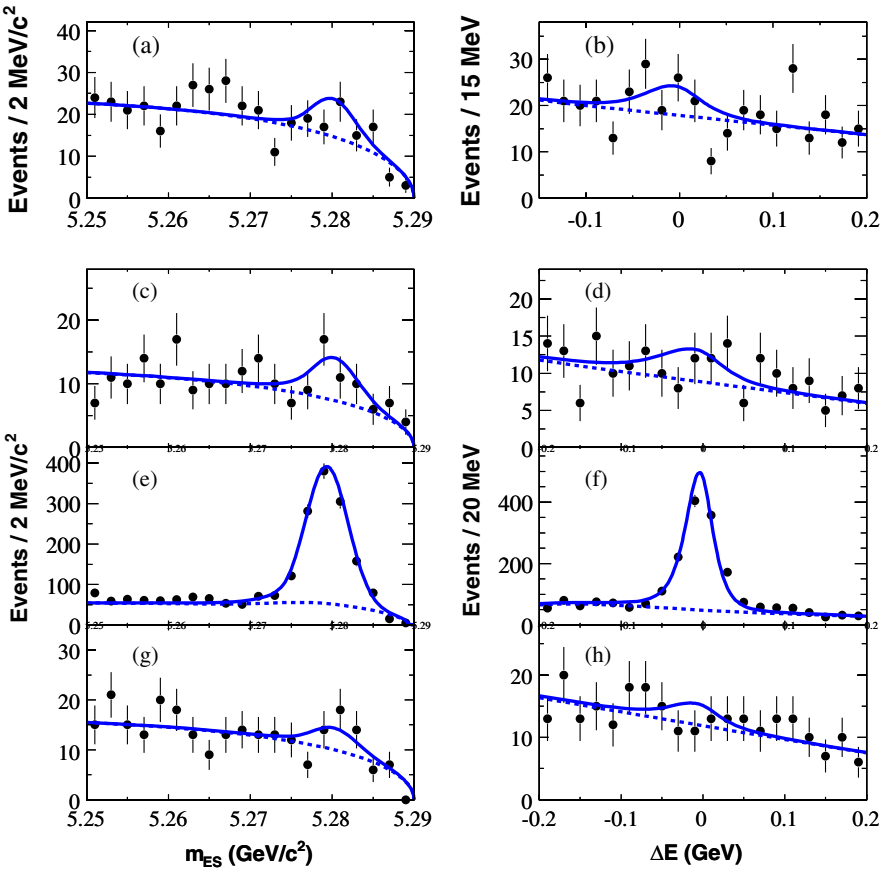

FIG. 2 (color online). The B^0 candidate $m_{\rm ES}$ and ΔE projections for ηK^0_S [(a), (b)], $\eta\omega$ [(c), (d)], $\eta' K^0_S$ [(e), (f)], and $\eta'\omega$ [(g), (h)] decays, with subdecays combined. Points with errors represent the data, solid curves the full fit functions, and dashed curves the background functions.

tion (0–12 events). The ML fit bias systematic error is taken to be half of the bias, summed in quadrature with its statistical uncertainty. The uncertainties related to the PDF parameterization are obtained by varying the PDF parameters within their errors. Published world averages [21] provide the uncertainties of the B-daughter branching fractions (0–4)%. These uncertainties are the main contribution to the systematic errors of the $B \to \eta' K$ decay modes. The uncertainty on $N_{B\bar{B}}$ is 1.1%. Other sources of systematic uncertainty are track (1%) and neutral particle (3–6)% reconstruction efficiencies; selection efficiency uncertainties are 1% each for the $\cos\theta_{\rm T}$ and PID requirements. Using large inclusive kaon and B decay samples we estimate a systematic uncertainty for $\mathcal{A}_{\rm ch}$ of 0.005 due to the dependence of the reconstruction efficiency on the charge of the high momentum $K^{\pm}$. Other sources of systematic uncertainties for $\mathcal{A}_{\rm ch}$ are the fit bias (0–0.02) and the presence of a fit bias in the signal yield (0.02–0.03). The systematic uncertainty due to fixing the value of the charge asymmetry in $B\bar{B}$ background components is taken to be the largest deviation observed when varying this value of $\pm 10\%$, and is in range (0–0.02).

In summary we present updated measurements of branching fractions for eight B^0 and four B^+ decays to charmless meson pairs. The results shown in Tables II and III are consistent with, but generally more precise than, previous measurements [2,3] and supersede our previous ones [2]. The branching fraction results are in agreement with predictions within the theoretical uncertainties that limit discrimination between different models [4–10]. We find evidence for three B^0 decay modes: ηK^0 (3.5σ), $\eta\omega$ (3.7σ) and $\eta'\omega$ (3.6σ). In the decay mode $B^+ \to \eta K^+$ we find evidence at 3.3σ for nonzero charge asymmetry, in agreement with theoretical predictions [6,9,19]. Discrimination between QCD factorization [6] and flavor SU(3) [9] symmetry models, based on the relative sign of the charge asymmetry in $B^+ \to \eta K^+$ and $B^+ \to \eta' K^+$ decays, is limited by the accuracy of the latter measurement. The measurement of $\mathcal{A}_{\rm ch}$ for $\eta'\pi^+$ shows a slightly better agreement with the QCD factorization prediction [6] than with the flavor SU(3) symmetry based model [9], within large theoretical and experimental uncertainties.

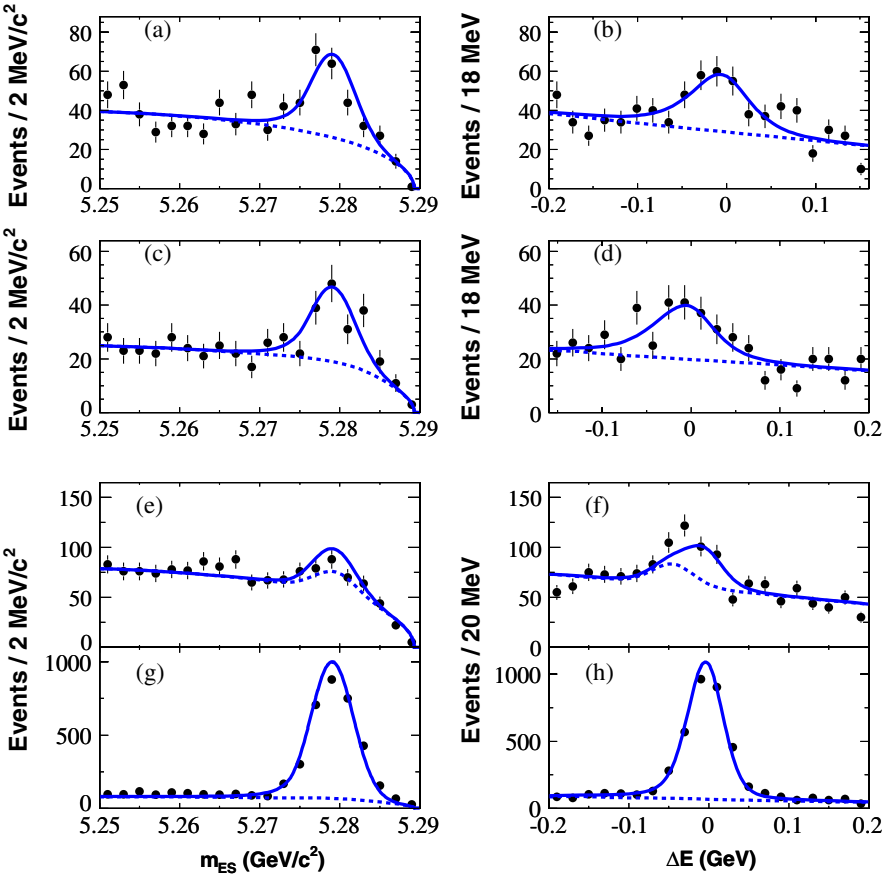

FIG. 3 (color online). The B^+ candidate $m_{\rm ES}$ and ΔE projections for $\eta\pi^+$ [(a), (b)], ηK^+ [(c), (d)], $\eta'\pi^+$ [(e), (f)], and $\eta' K^+$ [(g), (h)] decays, with subdecays combined. Points with errors represent the data, solid curves the full fit functions, and dashed curves the background functions.

We are grateful for the extraordinary contributions of our PEP-II colleagues in achieving the excellent luminosity and machine conditions that have made this work possible. The success of this project also relies critically on the expertise and dedication of the computing organizations that support *BABAR*. The collaborating institutions wish to thank SLAC for its support and the kind hospitality extended to them. This work is supported by the U.S. Department of Energy and National Science Foundation, the Natural Sciences and Engineering Research Council (Canada), the Commissariat à l'Energie Atomique and Institut National de Physique Nucléaire et de Physique des Particules (France), the Bundesministerium für Bildung und Forschung and Deutsche Forschungsgemeinschaft (Germany), the Istituto Nazionale di Fisica Nucleare (Italy), the Foundation for Fundamental Research on Matter (The Netherlands), the Research Council of Norway, the Ministry of Education and Science of the Russian Federation, Ministerio de Educación y Ciencia (Spain), and the Science and Technology Facilities Council (United Kingdom). Individuals have received support from the Marie-Curie IEF program (European Union) and the A. P. Sloan Foundation.

[1] Charge conjugation is implied throughout this paper.
[2] B. Aubert *et al.* (*BABAR* Collaboration), Phys. Rev. Lett. **93**, 181806 (2004); Phys. Rev. D **74**, 051106 (2006); **76**, 031103 (2007).
[3] J. Schümann *et al.* (Belle Collaboration), Phys. Rev. Lett. **97**, 061802 (2006); P. Chang *et al.* (Belle Collaboration), Phys. Rev. D **75**, 071104(R) (2007); J. Schümann *et al.* (Belle Collaboration), Phys. Rev. D **75**, 092002 (2007).
[4] M. Bauer *et al.*, Z. Phys. C **34**, 103 (1987); A. Ali and C. Greub, Phys. Rev. D **57**, 2996 (1998); A. Ali, G. Kramer, and C. D. Lu, Phys. Rev. D **58**, 094009 (1998); Y. H. Chen *et al.*, Phys. Rev. D **60**, 094014 (1999); J.-H. Jang *et al.*,

Phys. Rev. D **59**, 034025 (1999).

[5] G. P. Lepage and S. J. Brodsky, Phys. Rev. D **22**, 2157 (1980); J. Botts and G. Sterman, Nucl. Phys. **B325**, 62 (1989); Y. Y. Keum *et al.*, Phys. Lett. B **504**, 6 (2001); Phys. Rev. D **63**, 054008 (2001); Y. Y. Keum and H. N. Li, Phys. Rev. D **63**, 074006 (2001); Z. Xiao *et al.*, Phys. Rev. D **75**, 014018 (2007) [and references therein].

[6] M. Beneke *et al.*, Phys. Rev. Lett. **83**, 1914 (1999); , Nucl. Phys. **B606**, 245 (2001);M. Beneke and M. Neubert, Nucl. Phys. **B651**, 225 (2003); **B675**, 333 (2003).

[7] C. W. Bauer *et al.*, Phys. Rev. D **63**, 014006 (2000); **63**, 114020 (2001); C. W. Bauer and I. W. Stewart, Phys. Lett. B **516**, 134 (2001); C. W. Bauer, in *Proceedings of the 4th International Conference on Flavor Physics and CP Violation (FPCP 2006), Vancouver, British Columbia, Canada, 2006*, eConf C060409, 039 (2006).

[8] H. K. Fu *et al.*, Phys. Rev. D **69**, 074002 (2004); Nucl. Phys. B, Proc. Suppl. **115**, 279 (2003).

[9] C. W. Chiang *et al.*, Phys. Rev. D **68**, 074012 (2003); **70**, 034020 (2004).

[10] C. W. Chiang *et al.*, Phys. Rev. D **69**, 034001 (2004).

[11] A. Datta and D. London, Phys. Lett. B **595**, 453 (2004); M. Ciuchini *et al.*, Phys. Rev. D **67**, 075016 (2003).

[12] M. Gronau and J. L. Rosner, Phys. Rev. D **53**, 2516 (1996); A. S. Dighe, M. Gronau, and J. L. Rosner, Phys. Rev. Lett. **79**, 4333 (1997); M. R. Ahmady, E. Kou, and A. Sugamoto, Phys. Rev. D **58**, 014015 (1998); D. Du, C. S. Kim, and Y. Yang, Phys. Lett. B **426**, 133 (1998).

[13] I. Halperin and A. R. Zhitnitsky, Phys. Rev. D **56**, 7247 (1997); E. V. Shuryak and A. R. Zhitnitsky, Phys. Rev. D **57**, 2001 (1998).

[14] A. R. Williamson and J. Zupan, Phys. Rev. D **74**, 014003 (2006) [and references therein].

[15] H. J. Lipkin, Phys. Lett. B **633**, 540 (2006).

[16] B. Aubert *et al.* (*BABAR* Collaboration), Phys. Rev. D **79**, 052003 (2009); Phys. Rev. Lett. **99**, 161802 (2007); K.-F. Chen *et al.* (Belle Collaboration), Phys. Rev. Lett. **98**, 031802 (2007).

[17] Y. Grossman *et al.*, Phys. Rev. D **68**, 015004 (2003); C. W. Chiang *et al.*, Phys. Rev. D **68**, 074012 (2003); M. Beneke *et al.*, Nucl. Phys. **B675**, 333 (2003); M. Gronau *et al.*, Phys. Lett. B **596**, 107 (2004); G. Engelhard *et al.*, Phys. Rev. D **72**, 075013 (2005).

[18] D. London and A. Soni, Phys. Lett. B **407**, 61 (1997).

[19] S. Barshay and G. Kreyerhoff, Phys. Lett. B **578**, 330 (2004).

[20] B. Aubert *et al.* (*BABAR* Collaboration), Nucl. Instrum. Methods Phys. Res., Sect. A **479**, 1 (2002).

[21] The Review of Particle Physics, C. Amsler *et al.*, Phys. Lett. B **667**, 1 (2008).

[22] The *BABAR* detector Monte Carlo simulation is based on GEANT4: S. Agostinelli *et al.*, Nucl. Instrum. Methods Phys. Res., Sect. A **506**, 250 (2003).

[23] W. D. Hulsbergen, Nucl. Instrum. Methods Phys. Res., Sect. A **552**, 566 (2005).

[24] R. A. Fisher, Annals of Eugenics **7**, 179 (1936).

[25] B. Aubert *et al.* (*BABAR* Collaboration), Phys. Rev. Lett. **94**, 161803 (2005).

[26] We use the function $f(x) = \exp(\frac{-(x-\mu)^2}{2\sigma_{L,R}^2+\alpha_{L,R}(x-\mu)^2})$, where μ is the peak position of the distribution, $\sigma_{L,R}$ are the left, right widths, respectively, and $\alpha_{L,R}$ are the left, right tail parameters.

[27] M. J. Oreglia, Ph.D. thesis, Stanford Linear Accelerator Center and Stanford University [SLAC Report No. SLAC-R-236, 1980, Appendix D]; J. E. Gaiser, Ph.D. thesis, Stanford Linear Accelerator Center and Stanford University [SLAC Report No. SLAC-R-255, 1982, Appendix F]; T. Skwarnicki, Ph.D. thesis, Cracow Institute of Nuclear Physics [DESY Report No. F31-86-02, 1986, Appendix E].

[28] H. Albrecht *et al.* (ARGUS Collaboration), Phys. Lett. B **241**, 278 (1990).